Some new developments in optical dynamic testing

Fu, Yu; Phua, Poh Boon

2009

Fu, Y., & Phua, P. B. (2009). Some new developments in optical dynamic testing. Fourth International Conference on Experimental Mechanics, 7522, pp.1-9.

https://hdl.handle.net/10356/91914

https://doi.org/10.1117/12.851414

Some new developments in optical dynamic testing

Y. Fu[1,*] and P. B. Phua[1,2]
[1]Temasek Laboratories & School of Physical and Mathematical Science, Nanyang Technological University, 50 Nanyang Drive, Singapore, 637553
[2]DSO National Laboratories, 20 Science Park Drive, Singapore 118230

ABSTRACT

In recent years, optical interferometry based on high-speed imaging has been applied to full-field, non-contact measurement of low-frequency vibration or continuous-deformation. Retrieving dynamic phase values from a sequence of interferogram leads to a precise measurement of different kinematic and deformation parameters of the testing object. However, the temporal measurement range of this type of 2-D method is still limited by the imaging rate of the camera. On the other hand, laser Doppler vibrometer (LDV) significantly extend measurement capabilities in time axis, but most of the present vibrometers are based on pointwise measurement. A scanning system is normally employed to generate a 2-D measurement. This will dramatically increase the measurement time and limit the system to study the repeatable events. In this paper, two new optical dynamic testing methods are introduced to increase the measurement range in temporal and spatial axes. One is based on high-speed digital holography from which the instantaneous phase can be retrieved spatially to avoid the phase ambiguity problem in temporal analysis. Another is a double-beam Doppler vibrometer which can measure the vibration on different points simultaneously. The results of these two methods show the trend that the optical interferometry will meet various requirements of dynamic measurement with different temporal and spatial resolutions.

Keywords: Spatio-temporal analysis, phase extraction, digital holography, vibration measurement, laser Doppler vibrometry, Fourier analysis.

1. INTRODUCTION

In the area of optical metrology, interferometry has been applied on dynamic measurement for many years. Generally there are two types of technique with different measurement ranges: (1) High-speed camera based optical interfeometry and (2) photo-detector (PD) based laser Doppler vibrometry. Both techniques enjoy the virtues of being noninvasive and high-accuracy, and are getting more widely used by industries. Even in 1990's, the first technique is applied on static measurement due to the limited imaging rate of the CCD camera. However, due to the rapid development of high-speed digital recording devices, it is now possible to record interferograms with rates exceeding 100,000 frames per second (fps). Retrieving precise spatial phase maps from these transient interferograms enables measurement of instantaneous 3-D profiles, deformations as well as dynamic responses. Different methods were reported to analyze this interferogram sequence [1-5]. Among them, the temporal phase analysis technique has the advantage of eliminating speckle noise, as it evaluates the phase pixel by pixel along the time axis. However, it does have a disadvantage: if only the intensity variations of pixels are analyzed, the determination of absolute sign of the phase is impossible. This limits the technique to the measurement of deformation in one known direction. Adding a temporal carrier [6] to the image acquisition process is a method to overcome these problems. However, the carrier frequency limits the measurement range of phase variation due to the constraints of Nyquist sampling theorem and the acquisition speed of the high-speed camera [7]. In order to avoid the carrier in time domain, the instantaneous phase has to be retrieved in spatial domain. Recently, a novel computer-aided optical technology, digital holography [8], has been successfully applied in different types of measurement. Due to the development of CCD, or CMOS sensors, and the capabilities of computers, now it is possible

* fuyuoptics@gmail.com;

Fourth International Conference on Experimental Mechanics, edited by C. Quan, K. Qian, A. Asundi, F. S. Chau,
Proc. of SPIE Vol. 7522, 752246 · © 2010 SPIE · CCC code: 0277-786X/10/$18 · doi: 10.1117/12.851414

to record holograms directly by a camera and to reconstruct the object digitally by a computer simulation. The result of the digital reconstruction is not only the amplitude of the object, but the phase of the object as well. This advantage makes digital holography more suitable for dynamic measurement. Pedrini [9] described a method for measuring dynamic events in which digital holograms of an object are recorded on a high-speed sensor and the phase of the wavefront recorded at different instants is calculated from the recorded intensity, by use of a 2-D digital Fourier transform method [10]. By unwrapping the phase in the temporal domain it is possible to get the displacement, including the direction of a vibrating object as a function of time. Previous investigation shows a combination of Fourier and windowed Fourier analysis [11-12] can be applied temporally to extract the instantaneous velocity and acceleration of the object [13]. Using this technique, a full-field measurement can be achieved on a vibrating object with low amplitude and/or frequency due to the limited measurement capabilities in time domain.

Compared to a full-field measurement by the technique mentioned above, photo-detector based laser Doppler vibrometry (LDV) [14] can only offer a point-wise measurement, but with large measurement range on vibration amplitude and frequency. On another word, large measurement range on velocity. The LDV is based on the Doppler effect that occurs when the laser light scatter from a moving surface and the interference between the measuring and a reference beam. It allows conversion of the instantaneous velocity of the object into the Doppler frequency shift. For the extraction of the Doppler frequency shift, different interferometric solutions can be used. The heterodyne as Mach-Zehnder and the homodyne as Michelson interferometer are two typical configurations. In order to measure the vibration at different points, LDV are equipped with a video camera and a scanning system (composed by two orthogonal mirrors). These Scanning Laser Doppler Vibrometers (SLDV) give the possibility of moving the measurement point rapidly and precisely on the testing surface, allowing the analysis of large surface with high spatial resolution. However, it is impossible to do the measurement simultaneously on different points. This drawback limits the system to study the repeatable events. In recent years, several types of multi-channel and multi-point LDV have been reported. Zheng [15] proposed a multichannel laser vibrometer based on a commercial Polytec vibrometer and an acousto-optic beam multiplexer. It is still a point-by-point measurement but only with a switch among different channels. Other multi-point vibrometers [16-18] are normally a combination of several sets of signal-point version, which dramatically increase the complexity of the system. Now high-frequency photo-detectors and high-speed data acquisition cards are available with the highest sampling rate of >10GS/s and the dynamic range of >10 bits. As we have enough frequency range for measurement, it is possible to encode vibration signals on different points into different frequency bands. Hence, multi-point vibration measurement is possible using one high-frequency photo-detector.

In this paper, two interferometric methods are applied in vibration measurement. One is a full-field vibration measurement on a miniature component using a high-speed-camera-based image-plane digital holographic microscopy. The capturing rate of the high-speed camera is only 500 frame/s. With such low imaging rate, the measurement can still be achieved on a vibration object with frequency of 50Hz and amplitude ~1 micron. The results show spatial carrier can remove the phase ambiguity of the vibration and increase the measurement range in time domain. The second application is a dual-point laser Doppler vibrometer using one high-speed photo-detector. The vibration signals are encoded into different frequency bands by two Acousto-optic modulators (AOMs). A one-dimensional signal is captured by a high-frequency photo-detector and digitized by an 8-bit high-speed acquisition card. The results show simultaneous measurement on different points can be realized by a LDV with single photo-detector.

2. VIBRATION MEASUREMENT BY DIGITAL HOLOGRAPHY

2.1 Image-plane digital holography

Figure 1 shows a schematic layout of the image-plane digital holographic microscopy which is sensitive to the out-of-plane displacement. The laser light is split into a beam for illumination of the object and a reference beam. The object beam illuminates a specimen with diffuse surface along a direction $\boldsymbol{e_i}$. Some light is scattered in the observation direction $\boldsymbol{e_o}$ where an image-plane hologram is formed on the CCD sensor as a result of the interference between the reference beam and the object beam. The reference beam is introduced by a single-mode optical fiber and is diverged toward the detector. Let $R(x,y)$ and $U(x,y)$ denote the reference and object waves, the intensity recorded on the CCD sensor can be expressed as

$$I_H(x,y) = |R_H(x,y)|^2 + |U_H(x,y)|^2 + R_H(x,y)U_H^*(x,y) + R_H^*(x,y)U_H(x,y) \quad (1)$$

where the subscript H indicated that these values are in the image plane and * denotes the complex conjugate. If $\theta_{\max}$ is the maximum angle between the object and reference beams, the maximum spatial frequency in the hologram is

$$f_{\max} = \frac{2}{\lambda}\sin\left(\frac{\theta_{\max}}{2}\right) \tag{2}$$

where λ is the wavelength of the laser. The experimental setup should be properly designed so that the Nyquist sampling theorem is satisfied over the full area of the detector, and in our case it is $f_{\max} < 1/(2\Delta)$, where Δ denotes the pixel size of the camera.

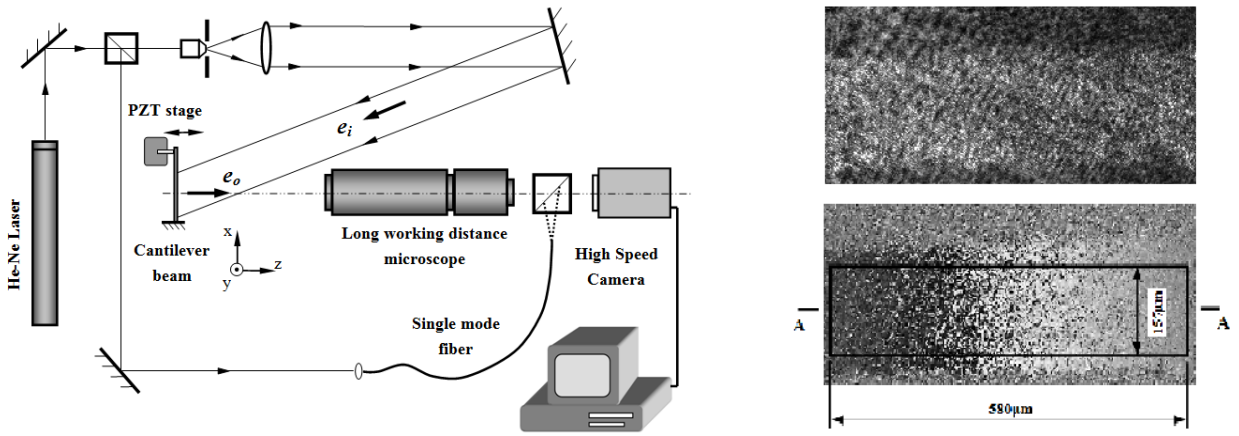

(a) (b)

Fig. 1 (a) Schematic layout of experimental setup; (b) The digital hologram captured and the phase reconstructed

The last two terms of Eq.(1) contain information of the amplitude and phase of the object wave. This information can be obtained by spatial filtering using the Fourier-transform method. The detailed description of Fourier evaluation of digital image-plane hologram can be found in Ref. 12. By taking the Fourier transform of the recorded intensity it is possible to filter out one of the last two terms in Eq.(1). After an inversed Fourier transform, the complex amplitude of the wavefront $U_H(x,y)$ is obtained. When a series of digital hologram is captured during the deformation or vibration of an object, a sequence of $U_H(x,y;t)$ is obtained. In this investigation, the obtained 3-D complex matrix is the original measurement data from which the displacement, velocity and acceleration of the testing object are evaluated.

It is well known that deformation of an object involves a change in the phase of the object beam. The relationship between the phase change $\Delta\phi = \phi_{t_2} - \phi_{t_1}$ and the out-of-plane displacement z is given by

$$\Delta\phi = \frac{2\pi z}{\lambda}\cdot \boldsymbol{S} \tag{3}$$

where $\boldsymbol{S} = \boldsymbol{e}_i - \boldsymbol{e}_o$ is the sensitivity vector given by the geometry of the setup, and $\boldsymbol{e}_i$ and $\boldsymbol{e}_o$ are the unit vectors of illumination and observation, respectively. The phase difference between two digital holograms recorded at t_1 and t_n can be calculated by

$$\Delta\phi = \arctan\frac{\mathrm{Im}\left(U(x,y;t_n)\cdot U^*(x,y;t_1)\right)}{\mathrm{Re}\left(U(x,y;t_n)\cdot U^*(x,y;t_1)\right)} \tag{4}$$

where Re and Im denote the real and imaginary parts respectively of the complex value. The $\Delta\phi$ obtained from Eq. (4) is within $[0,2\pi)$, and phase unwrapping in time axis allows the determination of the total displacement since the first frame of the measurement process, as opposed to the displacement relative to some other points in the field of view,

which is all that can be achieved with spatial unwrapping. If the first hologram is considered as a reference, we will have a series of $U(x,y;t_n)\cdot U^*(x,y;t_1)$ whose phase values after temporal unwrapping $\varphi(x,y;t_n)$ are proportional to the displacement at the instant t_n. In this application, two algorithms based on Fourier transform filtering and windowed Fourier ridge methods [11, 13] are applied spatio-temporally to evaluate the velocity and acceleration distributions along the cantilever beam. Here we omit the algorithms of windowed Fourier filtering and windowed Fourier ridge methods. Please refer to Ref. [19] for details.

2.2 Experimental illustration and results

The specimen tested in this study is a steel cantilever beam with a diffuse surface. The length, width and thickness of the beam are 1000, 200 and 100μm, respectively. The beam is subjected to a preload and a vibration with sinusoidal configuration at the free end by a PZT stage. The frequency of the vibration is around 50 Hz in this case. The beam of a He-Ne laser (Melles Griot, 05-LHP-927, Maximum 75mW at $\lambda = 632.8nm$) is divided into the object beam and reference beam. The cantilever beam is illuminated at an angle of 28° and is imaged at a right angle using a long working distance microscopic lens (OPTEM Zoom 100C, Numerical Aperture NA = 0.016 at image side with 6x magnification) by the sensor of a high-speed camera (KODAK Motion Corder Analyzer, SR-Ultra) with pixel size of $7.4\times7.4\mu m^2$. With this arrangement, a 1 *rad* phase change is equivalent to a 51.9 *nm* displacement in *z*-direction. The interference between the reference and object beams generates an image-plane hologram on the camera sensor. Two hundred holograms are captured with an imaging rate of 500 frames/s. The image size is 512×240 pixels and the imaging area is near the clamping end as shown in Fig. 1(b). Figure 1(b) also shows a typical wrapped phase map obtained by Eq. (4). The area of 480 ×130 pixels [as shown in Fig. 1(b)] has been selected to process.

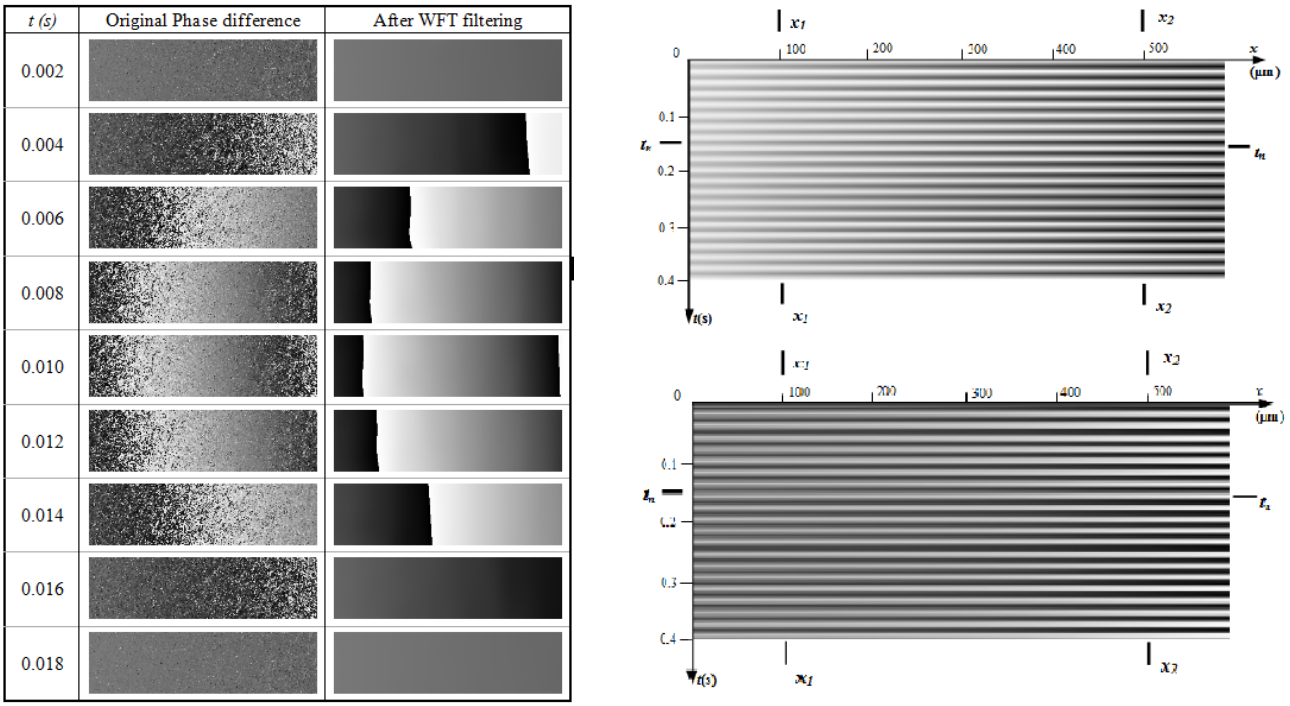

Fig. 2 (a) A sequence of original wrapped phase maps and the phase maps after WFT filtering; (b) Unwrapped phase maps shown the displacement and velocity variation in spatio-temporal plane.

The left column in Fig. 2(a) shows a series of original wrapped phase $\Delta\phi$ at different instants. The phase maps after 2-D WT filtering is shown in the right column. It is observed that the WFT filtering performs very well and a smooth wrapped phase is obtained. Similarly it is applied to all original wrapped phase maps. As the specimen measured

is a cantilever beam, and the displacements in *y*-direction are little varying, a cross section A-A [indicated in Fig. 1(b)] is selected to process. The temporal phase variations of A-A section generate a spatiotemporal distribution as shown in the first diagram of Fig. 4(b) which is proportional to the displacement of the beam. The phase values in Fig. 4(a) are then converted to the exponential values $\exp(j\cdot\Delta\phi)$ and processed by windowed Fourier ridge algorithm to extract the instantaneous velocity. The result is also shown in Fig 4(b) which is proportional to the velocity of the beam.

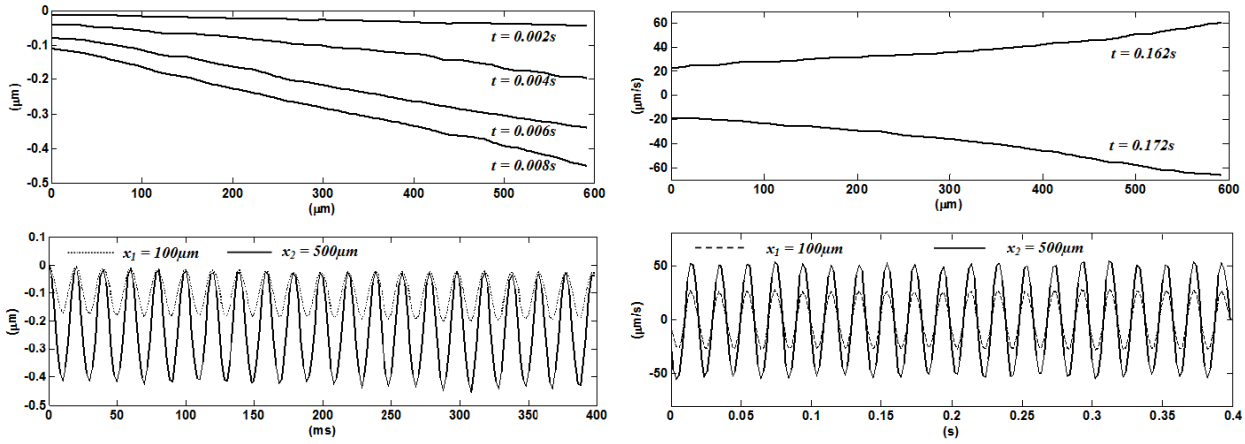

(a) (b)

Fig.3 Instantaneous (a) displacement and (b) velocity distributions along time and spatial axis (x-axis).

Figure 3(a) shows the displacement of the beam at different instants t_n and the displacement variation of two points, $x_1 = 100\mu m$ and $x_2 = 500\mu m$ from the left side of image, on the A-A line. Figure 3(b) shows two distributions of instantaneous velocities at $t = 0.162s$ and $t = 0.172s$, and the velocity variations of x_1 and x_2 on the line A-A. A similar process can be applied again to obtain the second derivatives in time axis.

It is noteworthy that the measurement range of the velocity and acceleration is limited due to the constraint of Nyquist sampling theorem and imaging rate of the high-speed camera. The maximum phase change between two adjacent frames is $\pm\pi$. However digital holography can extract the phase from one hologram, no phase ambiguity problem exists. It is not necessary to introduce the temporal carrier. Comparing to other optical interferometries such as ESPI and shearography, the vibration measurement range is tremendously enlarged with the absence of temporal carrier frequency.

3. VIBRATION MEASUREMENT BY MULTI-BEAM DOPPLER VIBROMETRY

3.1 Single and Multi-point Laser Doppler Vibrometer

When a laser beam with wavelength of λ is projected on an object moving with velocity $\boldsymbol{V}$, the shifted frequency f_D of the reflected laser beam is proportional to the velocity of the object due to the Doppler effect, and can be expressed as

$$f_D = \left|\frac{V\cdot S}{\lambda}\right| \tag{5}$$

where $\boldsymbol{S} = \boldsymbol{e}_i - \boldsymbol{e}_o$ is again the sensitivity vector given by the geometry of the setup, and $\boldsymbol{e}_i$ and $\boldsymbol{e}_o$ are the unit vectors of illumination and observation, respectively. $\boldsymbol{S}$ can be considered as 2 when the illumination and observation are approximately in right angle. In order to avoid the direction ambiguity problem in frequency shift, two typical solutions can be applied: the heterodyne Mach-Zehnder interferometer with one photo-detector and an AOM in one arm and homodyne Michelson interferometer with two photo-detectors. In the former technique two photo-detectors can detect signals with $\pi/2$ phase shifting, while the latter technique introduces a temporal carrier so that a frequency-modulated

(FM) signal is obtained. Both techniques have been applied in commercial LDVs. For multi-channel LDV, heterodyne Mach-Zehnder interferometer with AOM takes the advantages of avoiding the complexity of setup.

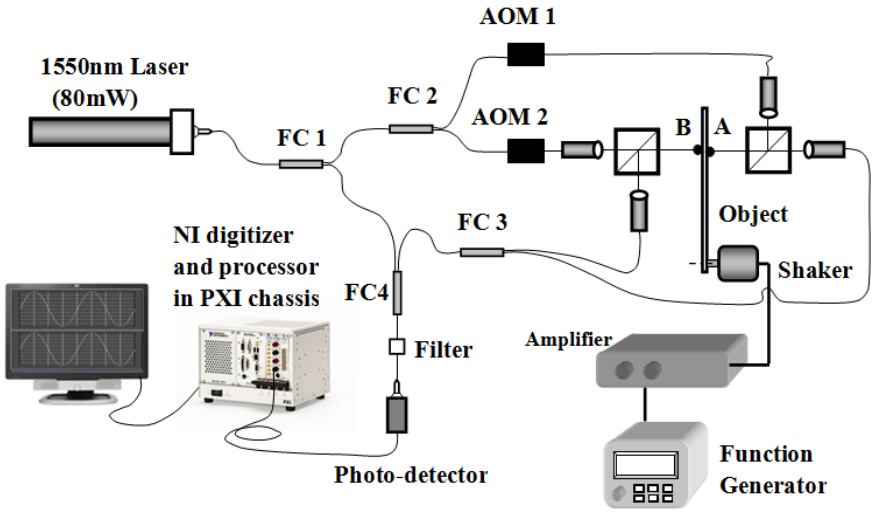

Fig. 4 Experimental setup on two-point laser vibrometer

3.2 Experimental illustration and result

Figure 4 shows the schematic layout of the proposed dual-point LDV. The beam of a DFB laser (Photonik, maximum 80mW at 1548.53nm in wavelength, linewidth <350kHz) is split into the object beam and reference beam by a fiber coupler (FC1, 99:1). The object beam is divided by another fiber coupler (FC2, 50:50) into two beams with different frequency shifting of 50MHz (AOM1) and 150MHz (AOM2), and these two beams illuminate a vibrating object at point A and B with a right angle. In this application, points A and B are located at the same location of the different sides of the vibrating beam, so that their vibrating amplitudes will be almost the same but with opposite phase changes. The specimen is a metallic beam with one end fixed on a shaker system. The amplitude and the frequency of the vibration are controlled by an amplifier and a function generator, respectively. In this experiment, a vibration of 185Hz has been applied on the object. The reflected beams are collected by two GRIN lens and combined with the reference beam by two fiber couplers (FC3 and FC4, 50:50). A bandpass filter of 1550nm is introduced to reduce the noise from other wavelength. The interference signal is captured by a high-frequency InGaAs photo-detector (Thorlabs, 5GHz, FC-coupled, Wavelength range of 900-1650nm). The signal is digitized by a high-speed acquisition card with sampling rate of 500MS/s (National Instruments, PXI 5154, Maximum sampling rate: 2GS/s) and processed by a PXI controller (National Instruments, PXI-8108, Core 2 Duo 2.53GHz).

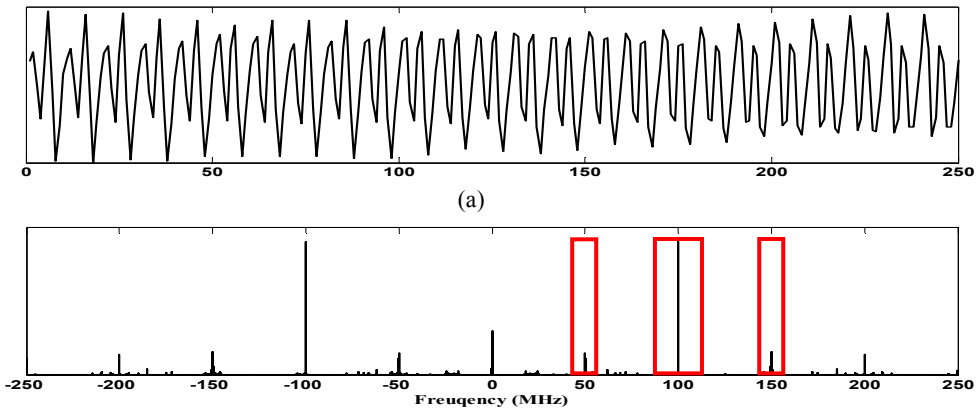

(a)

(b)

Fig. 5 (a) The original signal captured by NI high-speed digitizer; (b) spectrum of original signal.

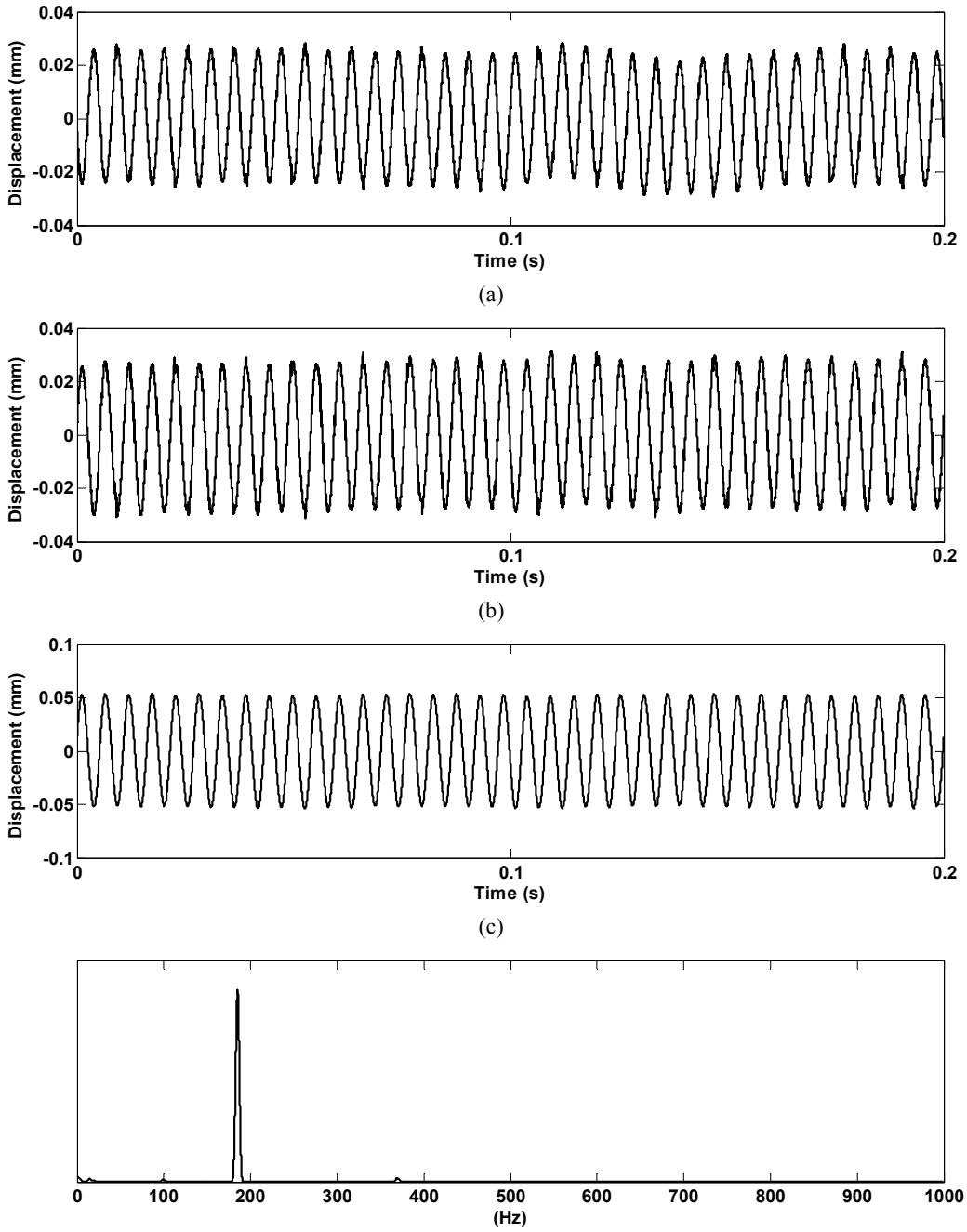

Fig. 6 Reconstructed vibration signals from bandpass filter centered at (a) 50MHz; (b) 150MHz; and (c) 100MHz; (d) Spectrum of reconstructed vibration signal with Zoom FFT.

A 1-D signal with 250M 8-bit data is obtained within 0.5 second. Figure 5(a) shows the voltage variation of the first 250 sampling points. Figure 5(b) shows the Fourier spectrum of the signal. Besides the DC term, several frequency components are observed. These components are centred at 50MHz (Due to the interference of 50MHz beam at point A and the reference beam), 150MHz (Due to the interference of 150MHz beam at point B and the reference beam) and 100MHz (Due to the cross-interference of 50MHz and 150MHz beams at points A and B), respectively. A bandpass filter and inverse Fourier transform is then applied at different frequency bands. After carrier removal, the absolute displacement variations on points A and B can be extracted as shown in Figs. 6(a) and 6(b). The vibrations at these two

points are almost the same in amplitude, but opposite in phase variation. Figure 6(d) is the spectrum of reconstructed vibration signal of point A obtained by zoom-FFT, which shows the object is vibrating with a frequency of 185Hz.

It is worth noting that the signal reconstructed from the frequency components centred at 100MHz (Fig. 6c) is the relative displacement between points A and B in this case. The amplitude of signal is the sum of displacements on points A and B, due to the opposite phase variation of these two points. This cross-interference among different points is useful in 2-point case. However, it may affect the results in multi-point measurement as it may contain the signal of several cross-interference among different points. Hence, the frequency bands of cross-interference among different points must be separated from the interference signals between different measurement points and the reference beam. It is possible but obviously will reduce the measurement range of velocity.

4. DISCUSSION AND CONCLUSION

The techniques shown in digital holography and laser Doppler vibrometer are all based on optical interferometry, although they have different measurement ranges of amplitude and frequency of vibration. The camera-based interferometer has sufficient sampling points in spatial domain but lower imaging rate on time axis. The measurement range of velocity is limited by the Nyquist sampling theorem ------ The maximum phase change between two adjacent frames is $\pm\pi$. In order to avoid the phase ambiguity in vibration measurement, carrier is necessary to applied in either temporal or spatial domain. In high-speed camera based optical interfeometry, as we have sufficient data points in spatial domain, carrier is more suitable to be introduced along spatial axes, and off-axis digital holography is a typical technique with spatial carrier. The instantaneous phase value on each pixel can be retrieved from one digital hologram. This will maximize the measurement range in temporal axis. On the other hand, the LDV has only one point in spatial domain, but with much higher capturing rate on time axis. The results of LDVs can be phase or the first derivative of the phase ------ frequency. Hence, it has large measurement range on the time axis and can meet the normal requirement from industries. However, pointwise measurement is an obvious disadvantage. Hence in this paper, we present a technique that encodes the vibration information of two spatial points into different frequency bands and captured by one photo-detector. The signal is then processed by Fourier analysis, and the vibration information at different points is extracted with different bandpass filters. The results show the vibration measurement can be done at different points simultaneously with one photo-detector. The trend in vibration measurement with optical interferometry shows that the above mentioned two techniques are developing in the same direction: a technique that has enough sampling points on both temporal and spatial domain so that they have the capability to cover the requirement at different measurement ranges.

The authors thank Mr. Min Guo of Temasek Laboratories @ Nanyang Technological University for the helpful discussion and his contribution in the experiment.

REFERENCES

[1] Takeda, M. Ina, H. and Kobayashi, S., "Fourier-transform method of fringe-pattern analysis for computer-based topography and interferometry," J. Opt. Soc. Am. 72, 156-160 (1982).

[2] Huntley, J. M., Kaufmann, G. H. and Kerr, D., "Phase-shifting dynamic speckle pattern interferometry at 1kHz," Appl. Opt. 38, 6556-6563 (1999).

[3] Huntley, J. M. and Saldner, H. "Temporal phase-unwrapping algorithm for automated interferogram analysis," Appl. Opt. 32, 3047-3052 (1993).

[4] Joenathan, C., Franze, B., Haible, P. and Tiziani H. J., "Speckle interferometry with temporal phase evaluation for measuring large-object deformation," Appl. Opt. 37, 2608-2614 (1998).

[5] Fu, Y., Tay. C. J., Quan, C. and Chen L. J. "Temporal wavelet analysis for deformation and velocity measurement in speckle interferometry," Opt. Eng. 43, 2780-2787 (2004).

[6] Kaufmann, G. H., "Phase measurement in temporal speckle pattern interferometry using the Fourier transform method with and without temporal carrier," Opt. Commun. 217, 141-149 (2003).

[7] Fu, Y., Tay, C. J., Quan, C. and Miao, H., "Wavelet analysis of speckle patterns with a temporal carrier," Appl. Opt. 44, 959-965 (2005).
[8] Goodman, J. W. and Lawrence R. W., "Digital image formation from electronically detected holograms," Appl. Phys. Lett. 11, 77-79 (1967).
[9] Pedrini, G. Osten, W. and Gusev, M. E., "High-speed digital holographic interferometry for vibration measurement," Appl. Opt. 45, 3456-3462 (2006).
[10] Fu, Y., Pedrini, G. and Osten, W., "Vibration measurement by temporal Fourier analyses of digital hologram sequence," Appl. Opt. 46, 5719-5727 (2007).
[11] Qian, K., "Two-dimensional windowed Fourier transform for fringe pattern analysis: Principles, applications and implementations," Opt. Laser Eng. 45, 304-317 (2007).
[12] Mallat, S., "A wavelet Tour of Signal Processing," Academic Press, San Diego, Calif. (1998).
[13] Fu, Y., Groves, R. M., Pedrini, G. And Osten W., "Kinematic and deformation parameter measurement by spatiotemporal analysis of an interferogram sequence," Appl. Opt. 46, 8645-8655, 2007.
[14] Castellini, P., Martarelli, M. and Tomasini E. P., "Laser Doppler Vibrometry: Development of advanced solutions answering to technology's needs," Mechanical Systems and Signal Processing, 20, 1265-1285 (2005).
[15] Zheng, W., Kruzelecky, R. V. and Changkakoki, R., "Multi-channel laser vibrometer and its applications," SPIE proceedings, 3411, 376-384, 1998.
[16] Di Sante, R. and Scalise, L., "Multipoint optical fiber vibrometer," Rev. Sci. Instrum., 73, 1321-1324, (2002).
[17] Di Sante, R. and Scalise, L., "A novel fiber optic sensor for multiple and simultaneous measurement of vibration velocity," Rev. Sci. Instrum., 75(6), 1952-1958, (2004).
[18] Dirckx, J. J. J. van Elburg, H. J., Decraemer, W. F., Buytaert, J. A. N. and Melkebeek J. A., " Performance and testing of a four channel high-resolution heterodyne interferometer," Opt. Lasers Eng. 47, 488-494, 2009.
[19] Fu, Y., Shi, H. and Miao, H., "Vibration measurement of miniature component by high-speed image-plane digital holographic microscopy," Appl. Opt. 48, 1990-1997 (2009).